

ACCEPTED MANUSCRIPT



Magnetosensitive neurons mediate geomagnetic orientation in *Caenorhabditis elegans*

Andrés Vidal-Gadea, Kristi Ward, Celia Beron, Navid Ghorashian, Sertan Gokce, Joshua Russell, Nicholas Truong, Adhishri Parikh, Otilia Gadea, Adela Ben-Yakar, Jonathan Pierce-Shimomura

DOI: <http://dx.doi.org/10.7554/eLife.07493>

Cite as: eLife 2015;10.7554/eLife.07493

Received: 15 March 2015

Accepted: 16 June 2015

Published: 17 June 2015

This PDF is the version of the article that was accepted for publication after peer review. Fully formatted HTML, PDF, and XML versions will be made available after technical processing, editing, and proofing.

Stay current on the latest in life science and biomedical research from eLife.
[Sign up for alerts](http://elife.elifesciences.org) at elife.elifesciences.org

1 **Magnetosensitive neurons mediate geomagnetic orientation in *Caenorhabditis***
2 ***elegans***

3

4 Andrés Vidal-Gadea^{1†}, Kristi Ward¹, Celia Beron¹, Navid Ghorashian², Sertan Gokce³, Joshua
5 Russell¹, Nicholas Truong¹, Adhishri Parikh¹, Otilia Gadea¹, Adela Ben-Yakar² & Jonathan
6 Pierce-Shimomura^{1*}

7

8 ¹Department of Neuroscience; Center for Brain, Behavior & Evolution; Center for Learning and Memory;
9 Waggoner Center for Alcohol and Addiction Research; Institute of Cell & Molecular Biology, The
10 University of Texas at Austin, Austin, TX, 78712.

11 ²Mechanical Engineering Department, The University of Texas at Austin, Austin, TX, 78712.

12 ³Electrical Engineering Department, The University of Texas at Austin, Austin, TX, 78712.

13 [†]Present address: School of Biological Sciences, Illinois State University, Normal, IL, 61790.

14 *To whom correspondence should be addressed. E-mail: jonps@austin.utexas.edu

15

16 **Running title:** Magnetic orientation in the nematode, *C. elegans*

17

18

19 **Summary**

20 Many organisms spanning from bacteria to mammals orient to the earth's magnetic
21 field. For a few animals, central neurons responsive to earth-strength magnetic fields
22 have been identified; however, magnetosensory neurons have yet to be identified in any
23 animal. We show that the nematode *Caenorhabditis elegans* orients to the earth's
24 magnetic field during vertical burrowing migrations. Well-fed worms migrated up, while
25 starved worms migrated down. Populations isolated from around the world, migrated at

26 angles to the magnetic vector that would optimize vertical translation in their native soil,
27 with northern- and southern-hemisphere worms displaying opposite migratory
28 preferences. Magnetic orientation and vertical migrations required the TAX-4 cyclic
29 nucleotide-gated ion channel in the AFD sensory neuron pair. Calcium imaging showed
30 that these neurons respond to magnetic fields even without synaptic input. *C. elegans*
31 may have adapted magnetic orientation to simplify their vertical burrowing migration by
32 reducing the orientation task from three dimensions to one.

33

34 **INTRODUCTION**

35 Many organisms such as birds, butterflies and turtles use the magnetic field of
36 the earth (geomagnetic field) to navigate across the globe (Johnsen and Lohmann,
37 2005, Guerra et al., 2014). Many animals migrate horizontally by preferentially using
38 either the horizontal (e.g. salmon, Quinn et al., 1981), or the vertical component of the
39 earth's field (e.g. turtles, Light et al., 1993). By contrast, magnetotactic bacteria use the
40 geomagnetic field to migrate roughly vertically by following the magnetic dip line
41 (Blackmore, 1975). Across hemispheres, magnetotactic bacteria reverse their polarity-
42 seeking preference, thus conserving the adaptiveness of the response (Blackmore et
43 al., 1980).

44 Although much is known about magnetosensation in bacteria, the cellular and
45 molecular basis for magnetosensation in animals is gaining in understanding. Recent
46 progress has been made identifying central neurons that respond to magnetic fields
47 (e.g. Wu and Dickman, 2012). Moreover, advancements have also been made
48 identifying candidate magnetosensory transduction mechanisms (e.g. Gegear et al.,

49 2010; Lauwers et al., 2013). Despite this progress, no magnetosensory neurons have
50 been identified in any animal (Edelman et al., 2015). Understanding how animals detect
51 and use magnetic fields will allow us to better predict the behavior of magnetosensitive
52 organisms, and will aid the study of how natural and artificial magnetic fields affect living
53 systems (Engels et al., 2014).

54 We show for the first time that the soil nematode *Caenorhabditis elegans* orients
55 to earth-strength magnetic fields. This ability is required for vertical burrowing migrations
56 directionally influenced by their satiation state. The direction and strength of the
57 behavioral response to magnetic fields of wild-type strains isolated around the world
58 correlated with their native magnetic field's inclination, and with the amplitude of the
59 field's vertical (but not its horizontal) component. The AFD sensory neurons respond to
60 earth-strength magnetic fields as observed by calcium imaging, and are necessary for
61 magnetic orientation, and for vertical migrations. Expression of the cyclic nucleotide-
62 gated ion channel, TAX-4, in AFD neurons is necessary for worms to engage in vertical
63 migrations, to orient to artificial magnetic fields, and for the AFD neurons to activate in
64 response to an earth-strength magnetic stimuli.

65 **RESULTS**

66 ***C. elegans* engages in vertical burrowing migrations**

67 While much is known about *C. elegans* crawling on agar surfaces, in the wild
68 worms likely spend most of their time burrowing through their substrate. After fifty years
69 of *C. elegans* research, studies looking at their burrowing behavior have only recently
70 begun (Kwon et al., 2013; Beron et al., 2015). Because worms are known to orient to a
71 variety of sensory stimuli that vary with depth in their native soil niches (Braakhekke et

72 al., 2013), we hypothesized that burrowing worms engage in vertical migrations like
73 magnetotactic bacteria. To test this, we placed worms in the center of 20-cm long, agar-
74 filled cylinders. Three layers of aluminum foil and a Faraday cage blocked light and
75 electric fields respectively from penetrating the cylinders. Pipettes were then aligned
76 horizontally in the 'north-south' or the 'east-west' directions, or vertically in the 'up-down'
77 direction in the absence of artificial magnetic fields (Figure 1A). Directional preference
78 during burrowing was quantified with a burrowing index computed as the difference
79 between the number of worms reaching either side divided by the total number of
80 worms reaching both sides. We found that when starved, the wild-type lab strain, N2,
81 originally from Bristol, England (Dougherty and Calhoun, 1948) preferentially migrated
82 down in vertically oriented cylinders, but did not show a burrowing preference when
83 cylinders were arranged horizontally (Figure 1B).

84 Most animals determine the up and down direction by sensing the gravitational
85 field of the earth (e.g. protozoans: Roberts, 2010; crustaceans: Cohen, 1955;
86 vertebrates: Popper and Lu, 2000). Alternatively, magnetotactic bacteria have been
87 shown to use the earth's magnetic field to migrate up or down within the water column
88 (Blackemore, 1975). To help distinguish magnetotactic versus gravitatic mechanisms
89 we built a magnetic coil system capable of producing homogeneous magnetic fields of
90 any desired 3D orientation (Figure 1-figure supplement 1). Our magnetic coil system is
91 comprised of three independently-powered, orthogonal Merritt coils that allow the
92 generation of magnetic fields of up to 3x earth strength (Figure 1-figure supplement 1,
93 Merritt et al., 1983). Within the 1-m³ coil system, a smaller 20-cm² Faraday cage, made
94 with copper fabric, protects the test volume from the electric field that is concomitantly

95 created alongside the magnetic field. Though often ignored in studies on animal
96 magnetic orientation, this precaution was necessary because *C. elegans* and other
97 animals exhibit strong behavioral responses to electric fields (Manière et al., 2011). We
98 repeated our vertical burrowing assay with an artificial magnetic field of earth-strength
99 oriented opposite to the local earth's magnetic field (i.e. magnetic north pointing up
100 rather than the natural orientation where magnetic north points down, Figure 1C). Under
101 these conditions, we expected that worms responding to gravitational cues would
102 continue to migrate down, while worms responding to magnetic cues would reverse
103 their direction and now migrate up. Consistent with magnetic stimuli dictating vertical
104 migration we found that starved N2 strain worms reversed their burrowing behavior and
105 migrated up (Figure 1B red bar).

106

107 ***C. elegans* orients to magnetic fields of earth strength in a satiation dependent** 108 **manner**

109 Our above results indicated that *C. elegans* might be able to detect and orient to
110 magnetic fields of earth strength. To further investigate how worms respond to magnetic
111 fields we placed them at the center of an agar plate and in turn placed this at the center
112 of our 1-m³ Merritt coil system (Figure 1-figure supplement 1; Figure 2A,B). We placed
113 an anesthetic (NaN₃) around the circumference of the plate, which allowed us to
114 immobilize and tally worms after they arrived at the plate's periphery. To determine if
115 the coil system generated an unwanted temperature gradient within the coil system, we
116 measured temperatures across the assay plate in response to a magnetic field (Figure
117 2-supplement 1A-B). Temperature gradients between the assay's start position (at the

118 center of the plate) and the finish position (at its edge) were negligible across time, and
119 did not vary significantly whether we imposed a magnetic field of one earth strength, or
120 if we cancelled out the earth's field by imposing a field of equal strength but opposite
121 direction (two-way repeated measures ANOVA, $N = 5$, $p = 0.123$).

122 First, as a control, we asked how worms respond when the earth's magnetic field
123 is cancelled. We accomplished this within the test volume of the magnetic coil system
124 using a magnetic field of equal strength and orientation to the field of the earth, but with
125 opposite direction. Worms in this regiment experienced a net magnetic field of
126 0.000 Gauss in three dimensions. Under this condition animals migrated randomly,
127 distributing evenly around the circumference of the assay plate (Figure 2C). We next
128 produced a homogeneous magnetic field of 0.325 Gauss (corresponding to half of
129 earth's maximum field intensity) directed across the assay plate. Worms assayed this
130 way showed a biased distribution directed $\sim 120^\circ$ to the imposed magnetic vector
131 (Figure 2D). Increasing the field strength to match the earth's maximum field strength
132 (0.650 Gauss) resulted in worms migrating approximately the same direction 132° to the
133 imposed vector (Figure 2E). Surprisingly, if worms were allowed to starve for just 30
134 minutes, they reversed their migratory distribution by $\sim 180^\circ$ to 305° relative to the field
135 vector (Figure 2F). These results demonstrate that *C. elegans* does not migrate simply
136 toward magnetic north like magnetotactic bacteria (Frankel et al., 2006); rather, they
137 display a preference to migrate at particular angles relative to magnetic north that
138 depend on feeding state. Similar plasticity for opposite migration preferences in *C.*
139 *elegans* has been documented for other sensory modalities (Bretscher et al., 2008;
140 Russell et al., 2014).

141 Do these seemingly arbitrary migratory angles serve a relevant purpose in the
142 worm's soil niche? As mentioned earlier, the standard wild-type *C. elegans* lab strain
143 (N2) was originally isolated in Bristol, England and cryogenically preserved there for
144 distribution of study around the world. We turned to available geomagnetic data from
145 NOAA to determine whether these migratory angles related to the earth's magnetic field
146 in England (Maus et al., 2009). In Bristol, the earth's magnetic vector enters the ground
147 (north pointing down) at approximately 66° of inclination (Figure 2G). Thus, in Bristol, to
148 optimally orient upward, a worm would need to migrate 156° to the magnetic field
149 penetrating the earth (green arc in Figures 2E and G); to optimally orient downward, a
150 worm would need to migrate 336° to the magnetic field (brown arc in Figures 2F and G).
151 To determine whether the preferred migratory angles of starved and well-fed worms in
152 our magnetic coil system assay matched these directions we performed a V test
153 (Batschelet, 1981). We found that the mean heading of fed worms (132°, N=1,268
154 animals) did not differ significantly from the upward direction for England (156.3°).
155 Likewise, the mean heading of starved worms (304.6°, N=1,079 animals) did not differ
156 significantly from the downward direction for England (336.3°). Please refer to
157 supplementary File 1a through 1e for descriptive and analytical statistics for all the data
158 presented in this study.

159 These results predicted that worms use the earth's magnetic field to migrate at
160 angles to the vector that would translate them up if they are fed, or down if they are
161 starved. To test this hypothesis, we placed well-fed or starved worms in vertically
162 arranged agar-filled pipettes away from artificial magnetic and electric fields as before.
163 We found that, consistent with this idea, starved worms preferentially migrated down

164 while well-fed worms migrated up (Figure 2G). These results are parsimonious with
165 *C. elegans* directing its vertical burrowing behavior by using the earth's geomagnetic
166 field. Soil nematodes feed on bacteria associated with rotting fruit on the soil surface
167 (Félix and Braendle, 2010) and on root rhizobacteria deep in the soil (Horiuchi et al.,
168 2005). Vertical migrations could be associated with travel between these distinct food
169 sources.

170

171 **Natural variation in magnetic orientation relates to geomagnetic inclination**

172 Like magnetotactic bacteria, *C. elegans* has been isolated across the world.
173 Magnetotactic bacteria from different hemispheres migrate in opposite directions to the
174 field vector. Bacteria that inhabit the northern hemisphere (where magnetic north points
175 down) are termed north-seeking magnetotactic bacteria, while those inhabiting the
176 southern hemisphere (where magnetic south points down) are termed south-seeking
177 magnetotactic bacteria (Frankel et al., 2006). The distribution of different wild-type *C.*
178 *elegans* isolates from around the world with distinct magnetic environments affords us a
179 valuable opportunity to investigate how animals in magnetically distinct environments
180 respond to magnetic fields. We therefore repeated our magnetic coil system and
181 burrowing assays with wild-type *C. elegans* worms isolated from Adelaide (Australia)
182 where the magnetic field of the earth is similar in strength and angle to that in England
183 but differs in the key respect of having the opposite polarity (Figure 3A). Unlike British
184 worms, we found that Australian worms placed in a plate within our magnetic coil
185 system migrated to an earth-strength field at 302.5° if fed, and 117.4° if starved. While
186 oriented oppositely in preference from the angles displayed by the British N2 strain,

187 these angles were similar in that they would also result in upward translation in Australia
188 for fed animals and down translation for starved ones (Figures 3B and C respectively).
189 To test if this response to an imposed artificial magnetic field reflected the migratory
190 burrowing preference of worm in a natural magnetic field, we compared the burrowing
191 behavior of Australian worms to that of the British strain. Paralleling our magnetic coil
192 system results, we found that in our lab (located in Texas, USA) Australian worms
193 migrated down when well-fed, and they migrated up when starved in the burrowing
194 assay (Figure 3D). Overall, these results suggest that unlike magnetotactic bacteria,
195 which follow magnetic field lines during their migrations, worms migrate at angles to the
196 imposed field that would result in optimal vertical translation in their native locations.

197

198 **Magnetotactic ability correlates with global field properties**

199 The results of our magnetic coil and burrowing experiments suggested that
200 worms use the local magnetic field to guide vertical migrations. Unfortunately these
201 experiments are limited to a few assays at the time, preventing their use in larger-scale
202 behavioral screens. To mitigate this shortcoming, we developed a new assay using
203 strong rare-earth magnets to quickly assess the ability of different strains to respond to
204 imposed magnetic fields (Figure 4A). This assay allowed us to run many assays at the
205 same time. Briefly, worms were placed at the center of an assay plate and allowed to
206 migrate freely (Figure 4A, and Methods). A magnet was then placed above one of two
207 equidistant “goal” areas. Magnetotactic performance was quantified with a magnetotaxis
208 index computed as the difference between the number of worms reaching either goal
209 divided by the number of worms reaching both goals. We found that when no magnet

210 was present, worms distributed evenly between these two goals. However, if the
211 magnet was present, worms preferentially migrated toward it (Figure 4-figure
212 supplement 1, Supplementary File 1a). To ensure the presence of the magnet did not
213 introduce an unwanted thermal gradient, we recorded the temperature difference
214 between goals in the presence and absence of a magnet and found that the two
215 treatments did not significantly differ from each other (Figure 2-figure supplement 1C,D).
216 We used this assay to compare the ability of different strains to detect and migrate in a
217 biased way in the presence of strong magnetic field. We first turned our attention to
218 many wild *C. elegans* strains isolated from different locations across the world.

219 The magnetic field of the earth varies greatly around the world (Maus et al.,
220 2009). If *C. elegans* uses the magnetic field for vertical migrations, what happens near
221 the equator where the vertical component of the earth's field is weakest? The global
222 heterogeneity in field characteristics made us wonder if selection pressure for
223 magnetosensation ability may drop off nearest the equator where the vertical
224 component of the magnetic field is at its weakest. To test this, we used our magnet
225 assay (Figure 4A) on wild-type populations isolated from ten locations across the planet
226 where the local magnetic field varies in inclination and vertical strength (Figure 4B, D,
227 Maus et al., 2009). We found that the ability of different worm populations to orient to an
228 artificial magnetic field was strongly correlated with the inclination (Figure 4B, C) and
229 vertical strength (Figure 4D, E) of the magnetic field at their native sites. The horizontal
230 component of the field, however, was a poor predictor of this magnetotactic ability
231 (Figure 4F). The strong correlation between magnetotaxis performance, local field
232 inclination, and vertical strength allowed us to successfully predict the magnetotaxis

233 index of an additional wild-type isolate from California, USA (Figure 4 red circle in
234 panels B-E, Supplementary File 1c). Wild-type isolates from equatorial locations where
235 the magnitude of the vertical component was close (or below) 0.2 Gauss, were either
236 unable or barely able to magnetotax (Supplementary File 1a). These results are
237 consistent with local adaptations to global magnetic field variations, and could perhaps
238 be used to model how other species may respond to temporal field variations (such as
239 magnetic polar drift or field reversals, Cox et al., 1964). We conclude from these results
240 that like many animals (Johnsen and Lohmann, 2005) *C. elegans* can use the magnetic
241 field's polarity and inclination to guide its migrations. Having determined that *C. elegans*
242 orients to magnetic fields, we turned our magnet assay to next investigate the cellular
243 and molecular underpinnings of this fascinating behavior.

244

245 **AFD sensory neurons are necessary for magnetic orientation**

246 To investigate the neuromolecular substrates for magnetosensation, we tested
247 mutants with deficiencies in a variety of previously characterized sensory pathways.
248 Mutants with severe defects in some sensory modalities displayed normal or nearly
249 normal magnetic orientation (Figure 5). These included worms deficient in the touch-
250 form of mechanosensation (*mec-10*, Arnadottir et al., 2011), light detection (*lite-1*,
251 Edwards et al., 2008), taste (*che-1*, Uchida et al., 2003), and oxygen sensation (*gcy-33*,
252 Zimmer et al., 2009). However, we also found mutants that were significantly impaired
253 in magnetotaxis. This group comprised worms with mutations in genes co-expressed in
254 a single sensory neuron pair called AFD, first implicated in thermosensation (Mori,
255 1999). These included two independent mutant alleles of *ttx-1*, important for AFD

256 differentiation, and the triple mutant lacking guanylyl cyclases, *gcy-23*, *gcy-8*, and *gcy-*
257 *18*, which together are critical for AFD function. Furthermore, we identified a set of
258 transduction mutants that failed to perform magnetic orientation. These included two
259 independent mutant alleles of each *tax-4* and *tax-2* genes. These encode subunits of a
260 cGMP-gated ion channel already implicated in sensory transduction in many sensory
261 neurons, including AFD (Komatsu et al., 1996).

262 To test the requirement of the AFD neuron pair in magnetosensation, we
263 genetically ablated them via cell-specific expression of a transgene for a human cell-
264 death caspase. One advantage of this technique is that only a fraction of individual
265 worms will inherit the artificial chromosome carrying the transgene. This allowed us to
266 compare the performance of sister worms grown and tested together under identical
267 conditions and only differing in having or not said transgene. After each assay,
268 individual worms with genetically ablated neurons were distinguished from their
269 unaffected sisters by the co-expression of a fluorescent transgene reporter. We found
270 that worms lacking the AFD sensory neurons failed to orient to an artificial magnetic
271 field, while their unaffected sisters oriented normally (Figure 6A, Supplementary File
272 1a). This could not be explained by non-specific defects, because these worms could
273 move and orient normally to olfactory stimuli (Figure 6-figure supplement 1). Similarly
274 ablating nearby sensory neuron pairs ASE and AWC had no effect on magnetotaxis.
275 The sensory ending of the AFD neurons consists of dozens of villi arranged anterior-to-
276 posterior (in an antenna-like formation) imbedded inside glial cells (Perkins et al., 1986).
277 Genetic ablation of the glia surrounding these structures, results in worms with viable
278 AFD neurons but lacking villi (Bacaj et al., 2008). These worms were unable to orient to

279 artificial magnetic fields (Figure 6A). This supports the idea that the villi may be the site
280 of magneto-transduction (and/or that the glia themselves contribute to this sense).
281 Taken together, our results demonstrate that the AFD sensory neurons are required for
282 magnetotaxis.

283

284 **TAX-4 cGMP-gated channel mediates magnetic orientation in the AFD neurons**

285 Many sensory neurons in *C. elegans* require the TAX-4 cGMP-channel for
286 sensory transduction (Komatsu et al., 1996). To determine if TAX-4 function in the AFD
287 neurons was sufficient for magnetic orientation, we selectively rescued expression of
288 *tax-4* in the AFDs neurons in a *tax-4* mutant background. Specific rescue of TAX-4 in
289 AFD neurons was sufficient to partially restore the ability of *tax-4(null)* mutant worms to
290 orient to an artificial magnetic field (Figure 6B, AFD+ others-). To investigate the
291 possibility that TAX-4 may also mediate magnetic orientation through additional neurons
292 we further rescued TAX-4 in all *tax-4*-expressing neurons by using its endogenous
293 promoter and regulatory elements. However, this did not result in an increased rescue
294 (Figure 6B, AFD+ others+). To test if *tax-4* contributed to magnetotaxis through any
295 other neuron asides from AFD, we tested *tax-4* mutants where this gene was rescued in
296 all *tax-4*-expressing neurons except for the AFD neurons (gift from Dr. R. Baumeister).
297 While rescuing *tax-4* in all but AFD neurons resulted in a rescue of the ability of these
298 animals to orient to chemical stimuli (Supplementary File 1a), these animals remained
299 unable to orient to magnetic fields (Figure 6B, AFD- others+).

300 These results support the hypothesis that the cGMP-gated ion channel TAX-4
301 plays an important role in the AFD sensory neurons for orientation to magnetic fields. To

302 confirm the relevance of these findings in a more natural magnetic assay, we retested
303 selected mutants under earth-like fields (in our coil system) and found similar results
304 (Figure 6C-E). The results above were obtained for animals orienting to artificial
305 magnetic fields. To determine if these results generalized to the ability of worms to
306 engage in vertical migrations we tested selected strains in our vertical burrowing assay
307 (without artificial magnetic field). Consistent with our observations in the magnet and in
308 the magnetic coil assays, *tax-4* mutant worms did not show preferential vertical
309 migration unless the gene was selectively rescued in the AFD neurons (Figure 6F).
310 Starved British and Australian wild-type isolates lacking the AFD neurons similarly failed
311 to engage in biased vertical migrations, although their sisters not carrying the transgene
312 (used to kill AFD) remained able to migrate down or up respectively (Figure 6F).

313

314 **The AFD neurons respond to earth-strength magnetic fields**

315 To determine whether the AFD neurons are directly responsive to magnetic
316 fields, we measured the fluorescence of a genetically encoded calcium indicator,
317 GCaMP3, in fully immobilized worms (Figure 7A, and Figure 7-figure supplement 1A).
318 After recording baseline activity (Figure 7B), we exposed mechanically immobilized
319 worms to an 8-sec, 65-Gauss (100x earth) rotating (2 Hz) magnetic stimulus (see
320 METHODS for details). We observed a transient increase in the average brightness of
321 the AFD neurons (Figure 7C). Successive stimuli consistently produced a reduced
322 response (Figure 7D). We observed a similar response when the magnetic stimulus was
323 decreased to 10x and 1x earth stimuli (6.5 and 0.65 Gauss respectively, Figure 7E and
324 F). To help determine if the AFD neurons themselves are magnetosensitive, and not

325 just synaptically downstream from “real” magnetoreceptive neuron(s), we measured
326 AFD calcium responses in worms impaired in rapid and dense-core synaptic
327 transmission (*unc-13* and *unc-31* mutant strains, Ahmed et al., 1992; Ann et al., 1997).
328 In the absence of chemical synaptic or neuromodulatory inputs, the AFD neurons
329 continued to respond to magnetic fields (Figure 7G, H). Qualitatively similar results (but
330 higher in amplitude) were observed for worms that were partially restrained (Figure
331 S5B). Magnetic-induced calcium responses in AFD were not observed in a *tax-4* mutant
332 background, suggesting that this requires Ca^{2+} entering the TAX-4 cGMP-gated ion
333 channel (Figure 7I, Figure 7-figure supplement 1B). Responses were also not observed
334 in an adjacent sensory neuron pair AWC (Figure 7J and Figure 7-figure supplement
335 1B). To quantitatively compare the magnetosensory response of AFD for different
336 conditions and mutant backgrounds, we plotted the average GCamp3.0 intensity during
337 the final 4 seconds of the magnetic stimulus relative to a 4-second baseline before
338 presentation of the stimulus (for the no-stimulus control we used the same time window
339 as for the other recordings). We found that the change in brightness was significantly
340 greater than control for all test conditions except in the case of *tax-4* mutant background
341 (Figure 7K). Our imaging results provide physiological evidence that the AFD sensory
342 neurons respond to magnetosensory stimuli relevant to geomagnetic orientation.

343

344 **DISCUSSION**

345 Here we provide the first behavioral and physiological evidence for
346 magnetosensory neurons. Nematodes unexpectedly appear to use the AFD neurons to
347 orient to earth-strength magnetic fields. *C. elegans* guides its vertical migrations using

348 the geomagnetic field and adjusts preference for up or down depending on their
349 satiation state. Population variability in magnetotactic ability correlates with global field
350 properties: with worms from locations where the field is strong and vertical
351 outperforming those where the field is weak and more horizontal. The AFD sensory
352 neuron pair is necessary for magnetic orientation and for vertical migrations. Similarly, a
353 cGMP-gated ion channel in the AFD neurons, TAX-4, is also necessary and sufficient
354 for these behaviors. The role of the AFD sensory neurons in magneto-transduction is
355 supported by their ability to respond to magnetic fields even in the absence of synaptic
356 inputs.

357

358 **Cellular and molecular substrates of magnetotransduction**

359 There are many possible ways in which the AFD neurons may play a role in
360 magnetic orientation. The magnetosensory AFD neurons also respond to temperature
361 (Mori, 1999), CO₂ (Bretscher et al., 2008), and moisture (Russell et al., 2014) gradients
362 in a satiation-dependent manner. All of these parameters vary with depth in the soil
363 (Jassal et al., 2005) supporting the role of the AFD neurons in vertical burrowing
364 migrations. Because *C. elegans* performs magnetotaxis in darkness (assays were
365 wrapped in 3-layers of foil), it is possible that it detects fields with nano-scale
366 compasses made of biological magnetic material previously described in *C. elegans*
367 (Cranfield et al., 2004), rather than by a light-dependent mechanism, although this study
368 did not investigate this possibility. However, based on our behavioral, mutant,
369 transgenic, and physiological analyses we hypothesize magnetic particles, perhaps
370 such as those found in magnetotactic bacteria (Frankel et al., 2006) and previously

371 reported in *C. elegans*, may (either directly or indirectly) be associated with the anterior
372 and posterior-directed microvilli of the AFD neurons. Magnetic stimulation of these
373 structures could lead to activation of unspecified guanylyl cyclases (such as GCY-8,
374 GCY-18, or GCY-23), in turn activating the TAX-4 channel and resulting in Na⁺ and Ca²⁺
375 influx and cell depolarization. These findings could represent an intriguing lead into the
376 putative magnetotransduction mechanism of the AFD neurons. It will be intriguing to
377 investigate whether the diverse range of other magnetotactic animals employ
378 magnetosensitive neurons with analogous morphology and transduction mechanisms
379 as the AFD neurons.

380

381 **Use of the earth's magnetic field in vertical migrations**

382 The magnetic field of the earth provides reliable directional and positional
383 information to organisms capable of its detection. Aside from magnetotactic bacteria,
384 magnetic orientation has been largely observed in animals that migrate horizontally
385 (Johnsen and Lohmann, 2005). Our finding that vertical migrations by an animal may
386 also be guided by this sensory modality opens a new niche for the study of magnetic
387 navigation. Magnetotactic bacteria passively migrate along field lines: with south-
388 seeking bacteria swimming down, and north-seeking bacteria swimming up in the
389 southern and northern hemispheres respectively (Frankel et al., 2006). Unlike bacteria,
390 *C. elegans* does not follow the field vector but rather migrates at an angle that appears
391 to maximize its vertical translation. The difference in migration angles and in response
392 amplitude between wild-type isolates from around the world suggests that this sensory

393 modality is under considerable selective pressure and will be the subject of future
394 studies.

395 Our findings that the direction of vertical migrations could be reversed by an
396 imposed magnetic field and that wild-type populations of worms from opposite
397 hemispheres displayed opposite vertical migration preference strongly suggests that *C.*
398 *elegans* relies on the geomagnetic field rather than gravity. Many organisms deduce
399 their vertical orientation by using the earth's gravitational field (gravitaxis). Studies on
400 paramecia suggest that the relative density of the organism against its media is
401 instrumental in gravitaxis (Kuroda and Kamiya, 1989). For terrestrial and marine
402 animals, the relative density of their media (air and water respectively) is largely
403 constant. However, for nearly buoyant worms imbedded in a soil matrix, the relative
404 density of their surrounding media is highly variable and may preclude reliance on
405 gravitaxis.

406 Many magnetotactic bacteria use a mechanism known as 'polar magneto-
407 aerotaxis' where these cells preferentially migrate up or down in chemically stratified
408 water or sediment columns using an single sensory pathway to integrate magnetotaxis
409 and aerotaxis (Blakemore et al., 1980; Popp et al., 2014). Like *C. elegans*, polar
410 magneto-aerotactic bacteria from different hemispheres have adapted their polarity
411 preference to match their native environment (Blakemore, 1975). It appears that the role
412 of magnetotaxis in *C. elegans*, as in bacteria, may be to increase the efficiency of taxis
413 to other sensory cues by reducing a search problem from three dimensions to one.
414 Unlike bacteria which migrate along the dip line at an angle relative to the vertical
415 direction, however, *C. elegans* appears to align motion at an angle to the magnetic field

416 that would enable a more vertical trajectory in its native environment. Our finding that
417 the strains from England, Australia and Hawaii each displayed a preferred magnetic
418 orientation preference that matched the geomagnetic field orientation at their source of
419 isolation rather than the one at the experimental site (Texas, USA) suggests a genetic
420 encoding of magnetic orientation preference.

421

422 **Magnetic orientation preference correlates with the physiological state attained**
423 **by the animals**

424 From previous work (Bretscher et al., 2008; Russell et al., 2014), it is clear that
425 satiation affects the sign of the response to sensory stimuli that the AFD neurons
426 respond to. However, our experiments did not provide evidence to answer why fed
427 worms migrate up and starved worms migrate down. One possibility concerns the
428 vertical stratification of food sources. *C. elegans* feeds bacteria growing on rotting fruit
429 on the soil's surface (Félix and Braendle, 2010), and on root rhizobacteria deep in the
430 soil (Horiuchi et al., 2005). Vertical migrations may direct travel between these
431 segregated food sources following the marginal value theorem (Carnov, 1976; Milward
432 et al., 2011). Rotting fruit on the surface represents an extremely rich, but transient,
433 food supply. By contrast, rhizobacteria represent a low-quality but stable source of food.
434 Surface populations likely grow exponentially until they exhaust their resources. For a
435 starved worm on the surface, burrowing down would be adaptive because it leads to
436 rhizobacteria in the plant roots. Rhizobacteria, however, represent a lower quality food
437 source. From here, fed worms may venture to emerge in search of better and more
438 plentiful food. Worms on poor diets have been shown to be more likely to abandon the

439 relative safety of their food patch in an attempt to find a higher quality source (Shtonda
440 and Avery, 2006). For these worms, an adaptive locomotor strategy would be to burrow
441 up in search of higher quality food sources, as burrowing down would not be likely to
442 result in finding a higher quality food patch. Future experimental studies will distinguish
443 between these and other possibilities by mimicking specific soil conditions.

444 Many animal species (including other nematodes, Prot, 1980) engage in vertical
445 soil migrations (Price and Benham, 1977). Therefore magnetic orientation may be more
446 widespread than previously believed. While the scale and nature of magnetosensation
447 make it challenging to study in large animals with extensive ranges, the small size,
448 genetic tractability, and research amenability of *C. elegans* make it an optimal model to
449 begin to unlock potentially conserved cellular-molecular mechanisms by which animals
450 detect and orient to the magnetic field of the earth.

451

452 **MATERIALS AND METHODS**

453 **Test Location.** All worms were raised and tested at The University of Texas at Austin,
454 Texas, USA (30° 20' N 97° 45' W) between 2011 and 2014. The local characteristics of
455 the magnetic field of the earth during the duration of the experiments were as follows:
456 Declination 4°35' to 4°13'(East); Inclination 59°19' to 59°12' (Down); Horizontal Intensity
457 0.245 to 0.244 Gauss; Vertical Intensity 0.413 to 0.410 Gauss (Down); Total Intensity
458 0.480 to 0.477 Gauss (Maus et al., 2009).

459 **Animals.** We conducted over 1,200 assays (>61,000 worms), averaging ~48 worms per
460 assay. All behavioral assays were conducted with experimenter blind to genotype of the
461 worms assayed. Because of the multimodal properties of the AFD neurons, assays

462 controlled for many physiological and environmental aspects prior to testing. To ensure
463 worms were in comparable physiological states, all assays were performed on (never
464 starved) day-one adult hermaphrodite *C. elegans*. Worms were never allowed to
465 overpopulate their plates. To minimize physiological changes due to unsealing of test
466 plates (e.g. altering the O₂/CO₂ ratio), worms were tested within 20 minutes of unsealing
467 their incubation plates. To test worms in comparable satiation states, worms tested
468 under the 'fed' status were assayed within ten minutes of being extracted from their
469 bacterial lawn. To test worms in the 'starved' state, we allowed worms to remain
470 suspended in liquid Nematode Growth Media (NGM) for 30 minutes prior to beginning
471 their run. Incubation temperature was between 19-21°C in standard NGM agar plates
472 seeded with *E. coli* (OP50) lawns (Brenner, 1974). Artificial magnetic fields were
473 removed from the vicinity of the worms, and the local field surrounding the worms was
474 determined to be of earth strength and direction with a DC Milligauss Meter Model MGM
475 magnetometer (AlphaLab, Utah, USA). To minimize novel background mutations, all
476 strains were tested within three months of thawing from cryopreserved stocks, with
477 additional re-thaws of fresh samples at three-month intervals.

478 **Genetic manipulations.** We used the GATEWAY system to generate transgenes for
479 transgenic strains (Hartley et al., 2000). Fluorescent reporters were used to identify
480 transgenic individuals (*Pmyo-2::mCherry*, *Pmyo-3::mCherry*, or *Punc-122::GFP*; see
481 Supplementary File 1e for specifics). We used the AFD-specific promoter (*Pgcy-8*) to
482 target the AFD neurons (Inada et al., 2006). To genetically ablate these neurons, we
483 constructed plasmids containing the human caspase gene *ICE* (gift from V. Maricq) and
484 transformed N2 wild-type worms to generate strains JPS264 *vxEx264[Pgcy-8::ICE]*.

485 Identical results were found for two independently derived strains, JPS265 and JPS271,
486 in a N2 background. AFD neurons were also killed in the Australian wild-type isolate
487 AB1 to generate strain JPS545 and JPS546. The ability of this transgene to kill the
488 AFD neurons was assessed by comparing GFP expression in the AFD neurons of
489 worms carrying the ICE construct, with that of worms not carrying it (Figure S4B, C). To
490 measure intracellular calcium levels in AFD neurons *in vivo* we expressed GCaMP3
491 (Tian et al., 2009, gift from L. Looger) *vxEx316[Pgcy-8::GCaMP3]* in *lite-1(ce314)*
492 worms to generate the strain JPS316. Identical results were found for three
493 independently derived strains, JPS275, JPS294, and JPS315. All of these strains were
494 capable of magnetosensation. We rescued *tax-4* specifically in AFD by constructing
495 plasmid with a wild-type copy of the *tax-4* cDNA (gift from Dr. Ikue Mori) expressed in
496 AFDs as described above to generate the strain JPS458 *tax-4(ks11) vxEx458[Pgcy-*
497 *8::tax-4(+)]*. Identical results were found for the independently derived strain, JPS459.
498 We also rescued with fosmid VRM069cE04 containing genomic region of *tax-4* with its
499 promoter, UTR and endogenous regulatory elements *vxEx458[VRM069cE04]* with
500 strain JPS458. *unc-13* or *unc-31* mutants were crossed with JPS316 males and F₂
501 worms were selected that exhibited GCaMP3 fluorescence and an uncoordinated
502 phenotype to generate strains JPS496 and JPS495 respectively. For details on the
503 construction of additional neuronal ablation strains please refer to the Extended Data
504 section in Russell *et al.* (2014).

505 **Magnetic response assays.** To determine if worms could sense and respond to
506 magnetic fields, we picked 50 never-starved (day-one) adults from an OP50 bacterial
507 lawn and into a 1- μ L drop of liquid nematode growth media (NGM). We used the latter

508 to clean the worms off bacteria, and to transfer worms to the center of a one-day old,
509 10-cm diameter, chemotaxis-agar assay plate. Equidistant from the worms, we drew
510 3.5-cm circles on either side and placed 1- μ L drops of 1-M NaN_3 at the center of these
511 circles to immobilize and count any worm that reached the area (Figure 4A). A N42
512 Neodymium 3.5-cm diameter magnet (K&J Magnetics Inc., Pennsylvania, USA) was
513 placed above one of the circles so that the assay plate was now traversed by a vertical
514 magnetic field gradient that became stronger toward the magnet and weaker away from
515 it. (Note that more commonly found weaker strength magnets produced qualitatively the
516 same behavioral results.) Worms were released from the liquid NGM droplet by wicking
517 excess liquid with filter paper. The total manipulation time (from bacterial lawn to the
518 beginning of the assay) was kept under ten minutes to avoid inadvertently starving the
519 worms. Worms released from the liquid NGM became able to freely migrate around the
520 plate. After 30 minutes we counted the number of worms NaN_3 -paralyzed in each circle
521 and calculated the magnetic orientation index (MI) as: $MI = (M-C)/(M+C)$. Where M is the
522 number of worms paralyzed within the magnet's circle, C is the number of worms
523 paralyzed within the control circle. We repeated the test a minimum of ten times for
524 each population (please refer to Supplementary Files 1a, c-e for the number of assays
525 and worms used in each experiment). The absence of artificial magnetic fields and
526 temperature gradients were empirically determined before each assay with DC
527 Milligauss Meter Model MGM magnetometer (AlphaLab, Utah, USA) and two high
528 accuracy Fisher thermometers accurate to 1/100 of a degree (Figure 2-figure
529 supplement 1E, F). Assays were run over multiple days and across a range of
530 temperatures (19-21 degrees Celsius). To ensure that unaccounted gradients in the

531 room did not affect the assays, we ran multiple assays in parallel. We arranged assay
532 plates so that their magnetic gradients were not aligned with one another or with the
533 magnetic field of the earth. In this configuration, the magnetic field on the plate surface
534 ranged between 40 and 2900 Gauss (Figure 4A).

535 To test if worms could perform magnetotaxis in the dark, we wrapped assay
536 plates in heavy-duty aluminum foil at least three layers thick. All burrowing experiments
537 were conducted similarly with the pipettes wrapped in multiple layers of aluminum foil.
538 All magnetic coil system experiments were conducted in the dark. Additionally,
539 burrowing and magnetic coil system experiments were conducted within an opaque
540 Faraday cage consisting of copper mesh.

541 **Magnetic coil system assays.** In order to test worms under earth-like homogeneous
542 magnetic fields we constructed a triple Merritt coil system (Merritt et al., 1983) of 1 m³ in
543 volume capable of generating a homogeneous magnetic field in the central 20 cm³ of
544 the space. A 22 cm³, copper fabric, Faraday cage around the test volume prevented
545 electric fields from interfering with our assays. Each of the three coil systems was
546 orthogonal to the other two (Figure 1-figure supplement 1) and was independently
547 powered by Maxtra Adjustable 30V 5A DC power supplies. We used a DC Milligauss
548 Meter Model MGM from Alphaslab Inc. (Utah, USA) to measure the magnetic field inside
549 the coil system before and after each experiment. Before the start of each experiment,
550 the system was used to neutralize the magnetic field of the earth within the coil system
551 by creating a field of equal strength and opposite orientation. A single 10-cm diameter,
552 agar-filled plate (Ward, 1973), with ~50 worms in its center, was placed in the center of
553 the coil system (Figure 1-figure supplement 1). To immobilize and count the worms that

554 reached the plate's edge, we placed a 10- μ l ring of 0.1-M NaN₃ anesthetic in the agar
555 around circumference of the plate. We next closed the Faraday cage and allowed the
556 worms to migrate freely within the plate with a homogeneous earth-strength (0.325 and
557 0.650 Gauss) magnetic field aligned with the plane of the assay plate. Alternatively, we
558 allowed worms to migrate in plates when the effective magnetic field inside the coil
559 system was 0.000 Gauss (earth-neutralized). After an hour, the angle at which each
560 worm had migrated with respect to the imposed field vector was recorded. To ensure
561 that the worms were responding to the generated magnetic field, and not to some
562 unknown gradient in the room, all assays were run in darkness with the direction of the
563 imposed magnetic field, and also the orientation of the magnetic coil system was varied
564 between trials with respect to the room and the earth's magnetic north. All experiments
565 were conducted blind with experimenter unaware of strain genotype.

566 In addition to magnetic and electric fields, the wires of coil system also produce a
567 small degree of heat. To test for the presence of unwanted temperature gradients we
568 used two high accuracy (0.01°C) thermometers (Fisher Scientific, New Hampshire) to
569 record the temperature at the center of the plates (where the worms begin the assay)
570 and at the edge of the plates (where they complete the assay). Please refer to
571 Supplementary File 1b for a summary of sample and population sizes, and for a
572 statistical description (and comparisons) of each dataset in the magnetic coil system
573 assays.

574 **Burrowing assays.** We filled 5-mL plastic pipettes with 3% chemotaxis agar and cut
575 and sealed the ends with Parafilm to minimize the formation of gaseous/humidity
576 gradients similar to our previous study (Beron et al., 2015). We made three equidistant

577 holes 10 cm apart in the pipettes. We injected 50 never-starved (day-one) adults into
578 the center hole, and 1.5 μ L 1-M of NaN₃ into the end holes to immobilize and easily
579 count the worms that reached either side. Worms were first picked from their incubation
580 plates into a 1- μ L liquid NMG solution and transferred within five minutes into the center
581 of the pipettes. Care was taken to ensure that worms were injected into solid agar
582 (rather than remaining suspended in liquid solution once injected). The genotype of the
583 strains was kept blind during the prep and running of the assay. The holes in the
584 pipettes were then sealed with Parafilm. We wrapped the pipettes in aluminum foil
585 multiple times (>3), to maintain the assays in complete darkness. Pipettes were aligned
586 horizontally, in either the north-south or the east-west direction, or vertically in the up-
587 down direction. Pipettes were placed inside a Faraday envelope made with copper cloth
588 to prevent electric fields from interfering with the assays. The assays were allowed to
589 run overnight and the worms immobilized at either end of the pipette were counted. The
590 burrowing index (BI) was calculated as: $BI = (A-B)/(A+B)$. Where A and B are the
591 number of worms on opposite ends of the assay pipette.

592 **Burrowing in artificial magnetic fields.** To assess if the surrounding magnetic field
593 could disrupt burrowing behavior, we arranged burrowing pipettes vertically inside the
594 magnetic coil system. We next generated a magnetic field of earth strength that had the
595 opposite inclination (magnetic north up) to the local magnetic field (magnetic north
596 down). Worms were allowed to burrow and their burrowing index was calculated as
597 described above.

598 **Temperature gradient assessment.** To determine if the presence of an artificial
599 magnetic field in the Merrit Coil System produced a temperature gradient in the assay

600 plate we used a Fisher High Accuracy thermometer sensitive to 0.01°C (Figure 2-figure
601 supplement 1). We placed one probe on the center of the plate (where worms begin the
602 assay) and one probe on the edge of the plate (where worms normally end the assay).
603 After closing the Faraday cage, and with the coil system off, we measured the
604 temperature on each probe in five minutes intervals for twenty minutes. At this point we
605 powered the cage on to produce either a horizontal magnetic field of 0.650 Gauss (1x
606 earth), or with a magnetic field able to cancel out the earth's own magnetic field inside
607 the cage (field cancelled). We continued to record the temperature of the probes every
608 ten minutes for one hour (the duration of a typical coil system experiment). We next
609 powered off the magnetic cage and once again recorded the temperature every five
610 minutes for an additional twenty minutes (Figure 2-figure supplement A, B).

611 To determine if the magnets placed above the plates in our magnet assays
612 produced a temperature gradient we placed temperature probes on the surface of the
613 agar above the test and control positions of agar plates as indicated in the magnet
614 assay procedure above. We compared the two temperature readings every ten minutes
615 for one hour (Figure 2-figure supplement C, D). To determine if temperature gradients
616 were created by the presence of a magnet we carried out these experiments both in the
617 presence and in the absence of a magnet. Between temperature experiments, the
618 thermal probes were immersed in a beaker containing 1L of dH₂O at the same distance
619 they had during the experiments to determine if their reading differed from one another
620 (Figure 2-figure supplement E, F).

621

622 **Testing genetically manipulated animals.** Worms carrying extrachromosomal arrays
623 with transgenes do not pass this construct to all their offspring. This permitted us to
624 blindly test clones that are identical in their genetics and in their upbringing, only
625 differing from one another in having (or not) the extrachromosomal array. In these
626 experiments, a mixed population of worms (both carrying and not carrying the array)
627 was tested together. After the assay, we used a fluorescent co-injection marker linked to
628 the transgene of interest to identify and count the number of worms belonging to each
629 population separately. We next calculated the magnetic orientation (or burrowing) index
630 for each subpopulation of worms. This ensured that the comparisons were made
631 between genetically identical populations that had grown under identical conditions,
632 their only difference being whether or not they carried the extrachromosomal array.
633 Expression of GCaMP3.0 did not interfere with ability to perform magnetotaxis to an
634 artificial magnet (Figure 7-figure supplement 1C).

635

636 **Calcium imaging in restrained animals.** Day-one adult wild-type (and mutant) worms
637 expressing the calcium-activity reporter GCaMP3 in neurons of interest were loaded
638 with liquid NGM into a microfluidic chip (Figure 7-figure supplement 1A). Worms were
639 immobilized and imaged in an Olympus BX51 scope at x60 magnification. Images were
640 sampled at 3.5-8 Hz using a CoolSNAP ES camera run by Windview 32. Each run
641 lasted 50 seconds and begun with a 12.5 second of baseline followed by the
642 presentation of a 6-seconds sinusoidal magnetic stimulus, and a 31.5-second recovery
643 period. Consecutive recordings were made 3-5 minutes apart. A N42 Neodymium 3.5-
644 cm diameter magnet (K&J Magnetics Inc., Pennsylvania, USA) was used to deliver the

645 magnetic stimulus. The intensity of the stimulus was calibrated with a DC Milligauss
646 Meter Model MGM magnetometer (AlphaLab, Utah, USA). The putative role of the
647 magnetic sensor in the worm is to detect the direction of the magnetic field. It therefore
648 follows that the cell must have an optimal stimulation angle between its sensor and the
649 surrounding field. Because we could not infer what this optimal alignment angle may be,
650 we decided to rotate the stimulus vector throughout 360 degrees to ensure that each
651 worm was stimulated with its presumably optimal angle. We did this by rotating the
652 magnet along the xy plane followed by the xz plane at a rate of 2 Hz. A series of TIFF
653 files was exported into ImageJ where the brightness of the cell body was measured
654 across each photo series. The average soma brightness accounting for bleaching was
655 calculated as previously described (Kerr, 2006).

656

657 **Calcium imaging in partially restrained animals.** Worms expressing GCaMP3 were
658 incubated as described above and placed along with 3- μ L liquid NGM on a 10% agar
659 pad on a microscope slide with the coverslip pressed down to inhibit swimming, but
660 permit slow crawling. Neurons were only imaged when the cells remained in the focal
661 plane for the duration of the experiment. We placed the slide in an upright Olympus
662 BX53 microscope equipped with and Retiga 2000R Fast 1394 camera (Q-Imaging, BC,
663 Canada). Worms were illuminated with a Series 1200 UV light source (X-cite,
664 Cincinnati, Ohio). We took a series of four pictures before, during, and after exposing
665 the setup, for ten seconds, to a 60 Gauss magnetic field generated by a Neodymium
666 magnet. The Tiff files of the images were exported as 8-bit files. We used ImagePro 6.0
667 (MediaCybernetics, Rockville, MD) to measure the brightness of the soma in each

668 picture series. We averaged the eight images before and after magnet exposure and
669 compared this value to the average soma brightness of the four images taken during
670 magnet exposure. We reported the percent change in brightness of the test condition to
671 the average of before and after (Figure 7-figure supplement 1B).

672

673 **Image Manipulations.** All plots were graphed using SigmaPlot 12 (Aspire Software)
674 and Matlab R2013b (Mathworks). Multiple plates were assembled in CoreIDRAW X6
675 (Corel).

676

677 **Statistical analysis.** All bars correspond to means, and variation is given as SEM
678 throughout. Linear statistical analyses were performed using SigmaPlot 12 (Aspire
679 Software). Comparisons between different experimental groups were performed by
680 planned, two-tailed paired or unpaired *t*-tests to compare different groups that were
681 normally distributed. Differences between non-normally distributed groups (or groups
682 that failed the test of equal variance) were evaluated using the Mann-Whitney Ranked
683 Sum Test, and two way repeated measures ANOVA (Temperature experiments).
684 Correlations between parameters were determined using linear regressions and
685 assessed using Pearson product-moment correlation coefficients. Circular statistical
686 analyses (descriptive and comparative) were performed using a circular statistics
687 toolbox for Matlab 2013b (Berens, 2009). We tested the significance of mean directions
688 using Rayleigh tests, and for difference between vertical “up” or “down” direction and
689 the mean direction of the population using *V* tests (Batschelet, 1981). Throughout this
690 study, *P* values were reported using the convention: * $P < 0.05$, ** $P < 0.001$. Please

691 refer to Supplementary File 1a-1e for descriptive, and Supplementary 1a-1b for
692 comparative statistics.

693

694 **Author Contributions:**

695 J.P.-S. is the Principal Investigator and contributed to experimental design; writing of the
696 manuscript; and unrestrained GCaMP3 experiments. A.V.-G. contributed to
697 experimental design, all experiments, and manuscript writing. K.W. performed magnet
698 and magnetic coil system assays as well as coil system construction. C.B. contributed
699 to burrowing experiments and magnet assays. S.G. and N.G. contributed to calcium
700 imaging of immobilized worms. J.R. contributed to strain construction. N.T. contributed
701 to burrowing assays and magnet assays. C.B. contributed to burrowing assays. A.P.
702 carried out burrowing assays. O.G. performed temperature experiments. A.B.-Y.
703 Contributed to microfluidic chip design, and calcium imaging experiments.

704

705 **ACKNOWLEDGEMENTS**

706 We thank Drs. C. Bargmann, R. Baumeister, I. Mori, V. Maricq, S. Lockery, L. Looger,
707 and S. Shaham for strains and constructs; G. Thomas of the UT Austin Physics
708 Electronic shop for assistance with magnetic coil system design; J. Cohn for
709 transgenesis assistance. Some strains were provided by the Caenorhabditis Genetic
710 Center, which is funded by NIH Office of Research Infrastructure Programs (P40
711 OD010440) and the National Bioresource Project of Japan. Funding was provided by
712 UT Austin UR Fellowship to K.W. and by a NIH NINDS grant to J.P.-S.

713

714 **REFERENCES**

- 715 Ahmed, S., Maruyama, I.N., Kozma, R., Lee, J., Brenner, S., and Lim, L. (1992). The
716 *Caenorhabditis elegans unc-13* gene product is a phospholipid-dependent high-
717 affinity phorbol ester receptor. *Biochem. J.* 287, 995-9.
- 718 Ann, K., Kowalchyk, J.A., Loyet, K.M., and Martin, T.F. (1997) Novel Ca²⁺-binding
719 protein (CAPS) related to UNC-31 required for Ca²⁺-activated exocytosis. *J. Biol.*
720 *Chem.* 272, 19637-40.
- 721 Amadottir, J., O'Hagan, R., Chen, Y., Goodman, M.B., and Chalfie, M. (2011). The
722 DEG/ENaC protein MEC-10 regulates the transduction channel complex in
723 *Caenorhabditis elegans*. *J. Neurosci.* 31, 4580-4610.
- 724 Bacaj, T., Tevlin, M., and Shaham, S. (2008). Glia are essential for sensory organ
725 function in *C. elegans*. *Science* 322, 744-747.
- 726 Batschelet, E. (1981). Circular statistics in biology (Mathematics in biology). Academic
727 Press. 1-371.
- 728 Berens, P. (2009). CircStat: A Matlab toolbox for circular statistics. *J. Stat. Soft.* 31, 1-
729 10.
- 730 Beron, C., Vidal-Gadea, A.G., Cohn, J., Parikh, A., Hwang, G., Pierce-Shimomura, J.T.
731 (2015) The burrowing behavior of the nematode *Caenorhabditis elegans*: a new
732 assay for the study of neuromuscular disorders. *Genes Brain Behav.* 14:357-368.
- 733 Blakemore, R.P. (1975). Magnetotactic bacteria. *Science* 190, 377-379.
- 734 Blakemore, R.P., Frankel, R.B. and Kalmijn, A.J. (1980). South-seeking magnetotactic
735 bacteria in the south hemisphere. *Nature* 286, 384-385.

736 Braakhekke, M.C., Wutzler, T., Beer, C., Kattge, J., Schrumpf, M., Ahrens, B.,
737 Schönig, I., Hoosbeek, M.R., Kruijt, B., Kabat, P., and Reichstein, M. (2013).
738 Modeling the vertical soil organic matter profile using Bayesian parameters
739 estimation. *Biogeosciences* 10, 399-420.

740 Brenner, S. (1974). The genetics of *Caenorhabditis elegans*. *Genetics* 77, 71-94.

741 Bretscher, A.J., Busch, K.E., and de Bono, M.A. (2008). Carbon dioxide avoidance
742 behavior is integrated with responses to ambient oxygen and food in *Caenorhabditis*
743 *elegans*. *Proc. Nat. Acad. Sci. USA* 105, 8044-8049.

744 Bretscher, A.J., Kodama-Namba, E., Busch, K.E., Murphy, R.J., Soltesz, Z., Laurent,
745 P., and de Bono, M. (2011). Temperature, oxygen, and salt-sensing neurons in *C.*
746 *elegans* are carbon dioxide sensors that control avoidance behavior. *Neuron* 69,
747 1099-1113.

748 Carnov, E.L. (1976). Optimal foraging, the marginal value theorem. *Theor. Popul. Biol.*
749 9, 129-136.

750 Cohen, M.J. (1955). The function of the receptors in the statocyst of the lobster
751 *Homarus americanus*. *J. Physiol.* 130, 9-34

752 Cox, A., Doell, R.R., and Dalrymple, G.B. (1964). Reversals of the earth's magnetic
753 field. *Science* 144, 1537-1543.

754 Cranfield, C.G., Dawe, A., Karloukovski, V., Dunin-Borkowski, R.E., de Pomerai, D., and
755 Dobson, J. (2004). Biogenic magnetite in the nematode *Caenorhabditis elegans*.
756 *Proc. Roy. Soc. Lond. B (Suppl.)* 271, S436-S439.

757 Doroquez, D.B., Berciu, C., Anderson, J.R., Sengupta, P., and Nicasto, D. (2014). A
758 high-resolution morphological and ultrastructural map of anterior sensory cilia and
759 glia in *Caenorhabditis elegans*. *eLife* 3, e01948.

760 Dougherty, E.C., and Calhoun, H.G. (1948). Possible significance of free-living
761 nematodes in genetic research. *Nature* 161, 29.

762 Edelman, N.B., Fritz, T., Nimpf, S., Pichler, P., Lauwers, M., *et al.* No evidence for
763 intracellular magnetite in putative vertebrate magnetoreceptors identified by
764 magnetic screening. *PNAS* 112, 262-7.

765 Edwards, S.L., Charlie, N.K., Milfort, M.C., Brown, B.S., Gravlin, C.N., Knecht, J.E., and
766 Miller, K.G. (2008). A novel molecular solution for ultraviolet light detection in
767 *Caenorhabditis elegans*. *PLoS Biol.* 6, 10.1371/journal.pbio.0060198.

768 Engels, S., Schneider, N-L., Lefeldt, N., Hein, C.M., Zapka, M., Michalik, A., Elbers, D.,
769 Kittel, A., Hore, P.J., and Mouritsen, H. (2014). Anthropogenic electromagnetic noise
770 disrupts magnetic compass orientation in a migratory bird. *Nature* 509, 353-356.

771 Félix, M.A., and Braendle, C. (2010). The natural history of *Caenorhabditis elegans*.
772 *Curr. Biol.* 20, R965-969.

773 Frankel, R.B., Bazyinski, D.A., Johnson, M.S. and Taylor, B.L. (1997). Magneto-
774 aerotaxis in marine coccoid bacteria. *Biophys. J.* 73, 994-1000.

775 Frankel, R.B., Williams, T.J., and Bazyilinski, D.A. (2006). Magnetoreception and
776 magnetosomes in bacteria: Magneto-Aerotaxis. *Microbiol. Mono.* 3, eds Steinbüchel
777 A, Schüler D (Springer, Heidelberg), pp 2-24.

778 Gegear, R.J., Foley, L.E., Casselman, A. and Reppert, S.M. (2010) Animal
779 cryptochromes mediate magnetoreception by an unconventional photochemical
780 mechanism. *Nature*. 463, 804-807.

781 Guerra, P.A., Gegear, R.J. and Reppert, S.M. (2014) A magnetic compass aids
782 monarch butterfly migration. *Nat Commun*. 24, 4164.

783 Hartley, J.L., Temple, G.F., and Brasch, M.A. (2000). DNA cloning using *in vitro* site-
784 specific recombination. *Genome Res*. 10, 1788-1795.

785 Horiuchi, J.I., Prithiviraj, B., Bais, H.P., Kimball, B.A., and Vivanco, J.M. (2005). Soil
786 nematodes mediate positive interactions between legume plants and rhizobium
787 bacteria. *Planta* 222, 848-857.

788 Kwon, N., Pyo, J., Lee, S.J., Je, J.H. (2013) 3-D worm tracker for freely moving *C.*
789 *elegans*. *PLoS One* 8:e57484.

790 Inada, H., Ito, H., Satterlee, J., Sengupta, P., Matsumoto, and K., Mori, I. (2006).
791 Identification of guanylyl cyclases that function in thermosensory neurons of
792 *Caenorhabditis elegans*. *Genetics* 172, 2239-2252.

793 Jassal, R., Black, A., Novak, M., Morgenstern, K., Nestic, Z., and Gaumont-Guay, D.
794 (2005). Relationship between soil CO₂ concentrations and forest-floor CO₂ effluxes.
795 *Agric. For. Meteorol.* 130, 176-192.

796 Johnsen, S., and Lohmann, K.J. (2005). The physics and neurobiology of
797 magnetoreception. *Nat. Rev. Neurosci.* 6, 703-12.

798 Kerr, R.A. (2006). Intracellular Ca²⁺ imaging in *C. elegans*. *WormBook* 1-13.

799 Komatsu, H., Mori, I., Akaike, R., and Ohshima, Y.M. (1996). Mutations in a cyclic
800 nucleotide-gated channel lead to abnormal thermosensation and chemosensation in
801 *C. elegans*. *Neuron* 17, 707-718.

802 Kuroda, K., and Kamiya, N. (1989). Propulsive force of *Paramecium* as revealed by the
803 video centrifuge microscope. *Exp. Cell. Res.* 184, 268-272.

804 Lauwers M, Pichler P, Edelman NB, Resch GP, Ushakova L, Salzer MC, Heyers D,
805 Saunders M, Shaw J, Keays DA. (2013) An iron-rich organelle in the cuticular plate
806 of avian hair cells. *Curr Biol.* 23, 924-929.

807 Light, P., Salmon, M. and Lohmann, K.J. (1993). Geomagnetic orientation of loggerhead
808 sea turtles: evidence for an inclination compass. *J. Exp. Biol.* 182, 1-10.

809 Manière, X., Lebois, F., Matic, I., Ladoux, B., Di Meglio, J-M., Hersen, P. (2011).
810 Running Worms: *C. elegans* self-sorting by electrotaxis. *PLoS One.* 6,
811 10.1371/journal.pone.0016637.

812 Maus, S.S., Macmillan, S., McLean, S., Hamilton, B., Thomson, A., and Nair, M. (2009).
813 The US/UK World Magnetic Model for 2010-2015, Technical report, NOAA,
814 NESDIS/NGDC.

815 Merritt, R., Purcell, C., and Stroink, G. (1983). Uniform magnetic field produced by
816 three, four, and five square coils. *Rev. Sci. Instrum.* 54, 879-882.

817 Milward, K., Busch, K.E., Murphy, R.J., de Bono, M., and Olofsson, B. (2011). Neuronal
818 and molecular substrates for optimal foraging in *Caenorhabditis elegans*. *Proc. Natl.*
819 *Acad. Sci. USA* 108, 20672-20677.

820 Mori, I. (1999). Genetics of chemotaxis and thermotaxis in the nematode
821 *Caenorhabditis elegans*. *Annu. Rev. Genet.* 33, 399-422.

822 Perkins, L.A., Hedgecock, E.M., Thomson, J.N., and Culotti, J.G. (1986). Mutant
823 sensory cilia in the nematode *Caenorhabditis elegans*. *Dev. Biol.* 117, 456-487.

824 Price, D.W., and Benham, G.S.Jr. (1977). Vertical distribution of soil-inhabiting
825 microarthropods in an agricultural habitat in California. *Envir. Entomol.* 6, 575-580.

826 Popp, F., Armitage, J.P., Schüler, D. (2014). Polarity of bacterial magnetotaxis is
827 controlled by aerotaxis through a common sensory pathway. *Nat. Comm.* 5, DOI:
828 10.1038

829 Popper, A.N., and Lu, Z. (2000). Structure-function relationship in fish otolith organs.
830 *Fish. Res.* 46, 15-25.

831 Prot, J.C. (1980). Migration of plant-parasitic nematodes towards plant roots. *Revue.*
832 *Nématol.* 3, 305-318.

833 Quinn, T.P., Merrill, R.T. and Brannon, E.L. (1981). Magnetic field detection in sockeye
834 salmon. *J. Exp. Biol.* 217, 137-142.

835 Roberts, A.M. (2010). The mechanics of gravitaxis in *Paramecium*. *J. Exp. Biol.* 213,
836 4158-4162.

837 Russell J., Vidal-Gadea, A.G., Makay, A., Lanam, C., and Pierce-Shimomura, J.T.
838 (2014) Humidity sensation requires both mechanosensory and thermosensory
839 pathways in *C. elegans*. *Proc. Nat. Acad. Sci. USA* 111, 8269-8274.

840 Shtonda, B.B., and Avery, L. (2006). Dietary choice behavior in *Caenorhabditis elegans*.
841 *J. Exp. Biol.* 209, 89-102.

842 Tian, L., Hires, S.A., Mao, T., Huber, D., Chiappe, M.E., Chalasani, S.H., Petreanu, L.,
843 Akerboom, J., McKinney, S.A., Schreiter, E.R., Bargmann, C.I., Jayaraman, V.,

844 Svoboda, K., and Looger, L.L. (2009). Imaging neural activity in worms, flies, and
845 mice with improved GCaMP calcium indicators. *Nature Methods* 6, 876-881.

846 Uchida, O., Nakano, H., Koga, M., and Ohshima, Y. (2003). The *C. elegans che-1* gene
847 encodes a zinc finger transcription factor required for specification of the ASE
848 chemosensory neurons. *Development* 130, 1215-1224.

849 Ward, S. (1973). Chemotaxis in the nematode *Caenorhabditis elegans*: identification of
850 attractants and analysis of the response by use of mutants. *Proc. Nat. Acad. Sci.*
851 USA 70, 817-821.

852 White, J.G., Southgate, E., Thomson, J.N., and Brenner, S. (1986). The structure of the
853 nervous system of the nematode *Caenorhabditis elegans*. *Phil. Trans. Royal. Soc.*
854 London B 314, 1-340.

855 Wu, L.Q., and Dickman, J.D. (2012). Neural correlates of a magnetic sense. *Science*
856 336, 1054-1057.

857 Zimmer, M., Gray, J.M., Pokala, N., Chang, A.J., Karow, D.S., Marletta, M.A., Hudson,
858 M.L., Morton, D.B., Chronis, N., and Bargmann, C.I. (2009). Neurons detect
859 increases and decreases in oxygen levels using distinct guanylate cyclases. *Neuron*
860 61, 865-879.

861

862 **FIGURE LEGENDS**

863 **Figure 1. *C. elegans* engages in vertical migrations whose direction depends on**
864 **satiation state and global origin.** (A) To determine if *C. elegans* engaged in
865 burrowing migrations we injected worms into agar-filled pipettes aligned horizontally
866 (east-west and north-south), or vertically (up-down). Alternatively, we disrupted the local

867 magnetic field around vertical pipettes (where magnetic north is down), by reversing the
868 local field polarity (thus making magnetic north up) with a magnetic coil system. (B) Only
869 worms in pipettes aligned vertically displayed burrowing bias, preferentially migrating
870 down unless the local magnetic field polarity was reversed (red bar) with the help of a
871 magnetic coil system (C).

872

873 **Figure 2. Preferred magnetotaxis orientation to a spatially uniform, earth-strength**
874 **field depends on satiation state, and local field properties.** (A) The core of the earth
875 generates a magnetic field that bisects the ground at different angles across the planet.
876 The vertical component is strongest at the poles and weakest near the equator. (B) We
877 constructed a Faraday cage within a triple-coil magnetic coil system to test the response
878 of worms under earth-like magnetic conditions. Circular histograms show the average
879 percentage of worms migrating in each of 18 20-degree-wide headings. The radius of
880 each circle represents 10% of the tested population and the mean heading vector arrow
881 would be as long as the radius if every worm converged on one heading, and have zero
882 length if worms distributed randomly around the plate (see Figure 1-figure supplement
883 1B for explanation of circular plots). When the magnetic field around them was
884 cancelled *C. elegans* migrated randomly (C). (D) Worms migrated at an angle to an
885 imposed field when its amplitude was half maximum earth strength (0.325 Gauss). (E)
886 When exposed to a field equaling maximum earth strength (0.625 Gauss), worms
887 showed stronger orientation. (F) Starving the worms for 30 minutes resulted in animals
888 migrating in the opposite direction to their heading while fed. (G) Burrowing worms
889 mirrored the magnetic coil results with fed worms preferentially burrowing up while

890 starved worms preferentially migrated down. For the standard lab strain N2 (native to
891 Bristol, England) the virtual up and down direction is represented in the circular plots by
892 a green and brown dashed arch and was not found to vary significantly from the mean
893 heading angle of fed and starved worms respectively. For the magnetic coil assays
894 migration along the imposed field would translate animals towards the 0°/N signs.

895

896 **Figure 3. Magnetic orientation varies with satiation state and local field**
897 **properties.**

898 To investigate if worms from distinct locations around the world displayed different
899 magnetic orientations we tested *C. elegans* isolated from Adelaide (Australia) where the
900 magnetic field is similar to that of the lab strain (Bristol, England) in strength and
901 inclination but opposite in polarity (A). Worms from Australia showed a magnetotactic
902 response reversed from the British strain. Plots for well-fed (B) and starved (C) worms
903 are shown and the local angle relative to the up and down direction are shown as green
904 and brown dashed arches respectively. For each population, the radius of the circle
905 represents 10% of the animals. The histograms show the percent of the worms that
906 migrated in each of 18 20-degree headings. The mean heading vector shows the
907 average direction of the animals and is equal to zero if all animals migrated randomly,
908 and to the circle radius if all animals migrate on a single heading. (D) We compared the
909 burrowing preference of fed and starved British and Australian worms placed in the local
910 (Texas) magnetic field and found that consistent with our magnetic cage experiments
911 both strains migrated in opposite directions.

912

913 **Figure 4. Magnetotactic variability between wild *C. elegans* isolates result from**
914 **differences in local magnetic field properties.**

915 (A) We developed a novel assay to rapidly assess the ability of worms to detect and
916 orient to magnetic fields. Worms placed at the center of a test plate were allowed to
917 migrate freely toward or away from a magnet. The number of animals by the magnet **M**,
918 or by a control area **C** were compared and used to calculate a magnetotaxis index:
919 $MI=(M-C)/(M+C)$. Wild-type *C. elegans* have been isolated across the planet at
920 locations with diverse local magnetic fields. (B) Earth's magnetic field inclination map
921 plotted from data obtained from NOAA (Maus et al., 2009) showing the isolation location
922 for twelve wild-type strains of *C. elegans* used in this study (circles). (C) The ability of
923 these wild isolates to magnetotax in our magnet assay strongly correlated with the
924 inclination of the magnetic field at their origin. We used the white ten isolates to
925 compute the correlation between these variables. This correlation was able to predict
926 the magnetotaxis index of an additional strain obtained from California (red circle). (D)
927 Map of the vertical component of the earth's magnetic field (Maus et al., 2009). (E)
928 Performance in the magnet assay was even more correlated with the vertical
929 component of the earth's magnetic field. However, the horizontal component of the
930 magnetic field (F) showed no correlation with the magnetotaxis index of the wild
931 isolates. The blue circle represents the lab strain (N2) from England. All assays
932 conducted at location indicated by the lone star. All values reported are means. Error
933 bars represent S.E.M.

934

935 **Figure 5. Geomagnetotaxis requires intact AFD sensory neurons.** We used our
936 magnet assay to test a large number of sensory mutants. Mutations that impair the
937 mechano- (*mec-10*), light- (*lite-1*), oxygen- (*gcy-33*), and taste- (*che-1*) sensory
938 pathways spared magnetotaxis, while mutations in genes specifically required for AFD
939 sensory neurons (*ttx-1* and *gcy-23,-8,-18*) abolished magnetotaxis. Mutations that
940 impair the cGMP-gated ion channel TAX-4/TAX-2 that are expressed in the AFD
941 sensory neurons (and other cells) similarly prevented magnetotaxis.

942

943 **Figure 6. Geomagnetotaxis requires the TAX-4/TAX-2 cGMP-gated ion channel in**
944 **the AFD sensory neurons.**

945 (A) Genetic ablation of the AFD neurons (or their sensory villi via ablation of amphid
946 glial cells) prevented magnetotaxis. However, ablation of adjacent sensory neurons
947 (ASE and AWC) did not impair this behavior. (B) Genetic rescue of the cGMP-gated ion
948 channel TAX-4 via cDNA specifically in the AFD neurons, or via genomic DNA in
949 additional *tax-4*-expressing neurons was sufficient to restore magnetotactic ability (white
950 bars) compared to their *tax-4*-mutant background controls (grey bars). However, rescue
951 of *tax-4* expressing neurons that excluded the AFD neurons failed to restore
952 magnetotactic behavior. We retested some of the mutants impaired in the magnet assay
953 in the magnetic coil system under earth-like fields. Impairment of the AFD neurons by
954 mutations in the *ttx-1* (C), *tax-2* (D), or *tax-4* (E) genes resulted in worms that failed to
955 orient to magnetic fields of earth strength (0.625 Gauss). Migration along the imposed
956 field would translate animals towards the 0°/N mark. (F) Genetic manipulations that
957 impaired (or rescued) magnetotaxis had a similar effect on geomagnetotaxis of vertically

958 burrowing worms. Starved British worms lacking the *tax-4* gene failed to burrow down.
959 However, control sister worms with the *tax-4* gene rescued specifically in the AFD
960 neurons (AFD+ others-) were able to burrow down. Conversely, starved British worms
961 lacking the AFD neurons (AFD dead) failed to migrate down, while control sister worms
962 (AFD alive) migrated down. Ablation of AFD in Australian worms similarly abolished
963 geomagnetotaxis. * $P < 0.05$, ** $P < 0.001$. All values reported are means, and error
964 bars represent S.E.M.

965

966 **Figure 7. The AFD sensory neurons respond to magnetic stimuli.** (A) Calcium
967 activity indicator GCaMP3 in the AFD neurons. (B) In the absence of a magnetic
968 stimulus the soma of AFD neurons rests at baseline. Exposing restrained worms to a
969 sinusoidal 65 Gauss (100x earth strength) magnetic stimulus caused the soma of the
970 AFD neurons to transiently increase brightness by 2% above baseline in response to
971 the first stimulus (C), and ~1% in response to subsequent stimuli (D). The AFD neurons
972 responded when the magnetic stimuli was reduced to 6.5 (E) and 0.65 Gauss (F, earth
973 strength). The AFD magnetic response remained even in synaptic mutants (G: *unc-13*
974 and H: *unc-31*) that render these cells synaptically isolated from other neurons. (I)
975 Animals lacking a functional copy of the *tax-4* gene did not show an increase in
976 brightness in response to a magnetic stimulus. (J) A 65 Gauss stimulus failed to elicit a
977 response in neighboring sensory neuron AWC. (K) The average soma brightness for the
978 final four seconds prior to stimulus, and the final four seconds of the stimulus were
979 compared. While the “no-stimulus”, the “*tax-4*”, and the “AWC” conditions resulted in no
980 significant brightness change, all other test conditions produced a significant increase in

981 AFD brightness above baseline. Change in relative fluorescence key for panels B-J
982 depicted in B with the exception of panel H which has its own key. N = 11 for B-D; 6 for
983 E-H; 14 for I; and 7 for K.

984

985 **SUPPLEMENTARY DATA**

986 **SUPPLEMENTARY TABLES**

987 **Supplementary File 1a.** Results of statistical comparisons between groups tested in
988 the magnet, burrowing, and chemotaxis assays. Comparisons appear in the order that
989 they were introduced in the text. Two-tailed *t*-tests were performed between normally
990 distributed groups that had equal variance to test the difference between the
991 populations' means. The Pearson product-moment correlation coefficient was used to
992 determine the correlation between variables. To test difference between means
993 belonging to non-normally distributed samples we used the non-parametric Mann-
994 Whitney ranked sum test. All statistic measures are from comparisons with the group
995 shaded in grey immediately above. Index refers to the mean (magnetic or burrowing)
996 index for each population (see Materials and Methods).

997

998 **Supplementary File 1b.** Summary of the magnetic coil system results for wild-type
999 animals from three different locations around the world and internal physiological status.
1000 Statistical tests were performed using the Circular Statistic toolbox for Matlab (Berens,
1001 2009). Comparisons between different parameters are shown within boxes.

1002

1003 **Supplementary File 1c.** Summary of local magnetic field properties and magnet assay
1004 results for wild-type worms from twelve different locations around the world (Figure 5).
1005 The exact isolation location for the LKC34 (Madagascar) strain is not known. We chose
1006 the northernmost location (Antisiranana) for the field properties, although choosing the
1007 southernmost location (Toliara) would not have yielded significantly different results.

1008

1009 **Supplementary File 1d.** Summary of the magnet-assay results for strains genetically
1010 modified to ablate (or to rescue gene function) in selected neurons (Figure 6).

1011

1012 **Supplementary File 1e.** Summary of the burrowing assay results (Figure 1-3, 6,
1013 8).

1014

1015 **SUPPLEMENTARY FIGURES**

1016 **Figure 1-figure supplement 1. Merritt coil system for 3D control of magnetic**
1017 **fields.** To expose worms to controlled and homogeneous earth-strength magnetic fields
1018 we constructed a triple magnetic Merritt coil system (Merritt et al., 1983). (A) Each
1019 system creates a magnetic field along the x (i), y (ii), and z (iii) directions and consists of
1020 four 1-m² squares, each arranged orthogonal to the other two. The system generates
1021 magnetic and electric fields. To prevent electric fields from affecting our experiments we
1022 built a Faraday cage around the experimental volume (iv). Dedicated DC power
1023 supplies for each coil (v) allowed us to control the orientation and the magnitude of the
1024 net magnetic field within the coil system. Assay plates (vi) were then placed inside the
1025 coil system for testing. We empirically calibrated the field within the coil system with the

1026 aid of a milligaussmeter (vii) from AlphaLab Inc. (Utah, USA). (B) In each magnetic coil
1027 system experiment, the north direction of the imposed magnetic field is signified by the
1028 0° on the top of the circular plot. Directly beneath this, and inside the circular plot, the
1029 strain's genetic background or geographic origin is indicated. The solid circular
1030 histograms represent the heading of the tested populations in a circle where the radius
1031 equals 10% of the entire population. Well-fed animals are represented by the black
1032 contour, while starved worms are represented by the grey contour. Circular plots had 18
1033 bins (20 degrees each). Similarly, the black and grey arrows represent the mean
1034 heading vector for the well-fed and starved populations respectively. The length of the
1035 vector is 0 if the population of animals migrated at random, and it is 1 if all animals
1036 migrate to a single point. The brown and green dashed curves indicate the heading that
1037 would result in (respectively) downward or upward translation at the original isolation
1038 site of each strain.

1039

1040 **Figure 2-figure supplement 1. Testing the presence of temperature gradients.** To
1041 determine if the artificial magnetic fields introduced unwanted temperature gradients in
1042 our assay we used high-accuracy thermometers capable of measuring 1/100 of a
1043 degree Celcius. (A) We recorded the temperature inside the coil system at the edge of
1044 the assay plate (where worms were tallied), and at the center of the assay plate (where
1045 worms began the experiment). We took temperature measurements under two
1046 magnetic regiments: when the earth's magnetic field was actively cancelled out inside
1047 the cage (0.000 Gauss, blue), and when we created an artificial magnetic field of earth
1048 strength inside the cage (0.650 Gauss, red). (B) The temperature difference between

1049 the center and the edge of the plate was reported every five minutes for thirty minutes
1050 before powering the cage on; every ten minutes for an hour while the cage was on; and
1051 every five minutes for thirty minutes after powering down the cage. A two-way repeated
1052 measures ANOVA failed to reveal significant differences between both treatments ($p =$
1053 0.123). (C) We measured the temperature difference between the end points of our
1054 magnet assays. Two temperature probes were placed at the target zones of magnet
1055 assay plates in the absence of a test magnet (blue), or when a magnet was present
1056 above one of the two test areas (red). (D) We report the difference between both
1057 temperature probes every ten minutes for one hour. A two-way repeated measures
1058 ANOVA failed to find a significant difference between the two experimental conditions (p
1059 = 0.559). (F) To empirically confirm that both probes were accurately calibrated we
1060 placed them inside a beaker containing 1 L of dH₂O and compared their readings
1061 between experiments. (F) Throughout our experiments both probes remained in
1062 agreement within 1/100th of a degree Celsius. In all experiments the two probes were
1063 positioned 5 cm apart.

1064

1065 **Figure 4-figure supplement 1. A new assay for testing magnetotactic ability. (A)**

1066 We developed a convenient assay able to determine the ability of worm populations to
1067 detect and orient to magnetic fields. Worms were placed in the center of an agar plate.
1068 A 1.5 μ l drop of anesthetic (NaN₃) was placed at the center of two test areas equidistant
1069 from the start, and a magnet was then centered above one of the two test areas. We
1070 calculated the magnetotaxis index as: Magnetotaxis Index= $(M-C)/(M+C)$. Where M is
1071 the number of worms found immobilized by the test area at the magnet, and C is the

1072 number of worms immobilized by the control test area. (B) If no magnet was present,
1073 worms distributed evenly between the two test areas. If a magnet was introduced above
1074 one of the areas, about two thirds of the worms preferentially migrated to the magnet
1075 test area. We repeated the experiment in assay plates wrapped in several layers of
1076 aluminum foil and observed that migration towards the magnet did not require light.

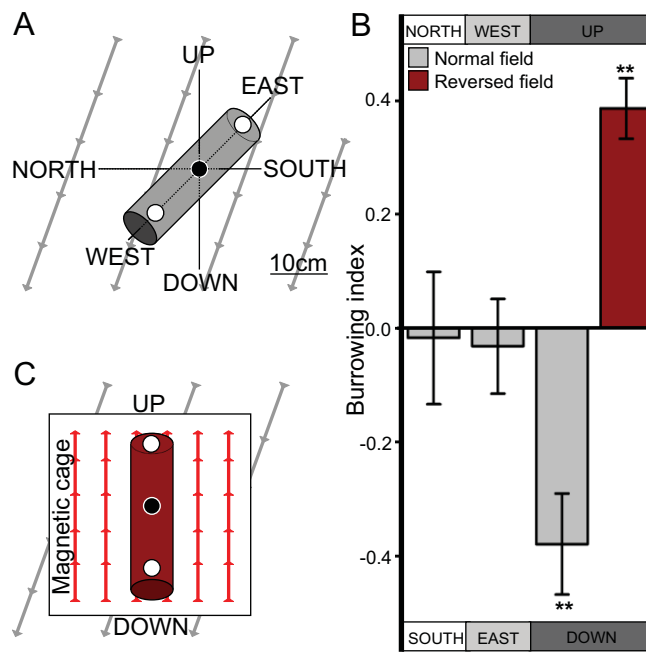
1077

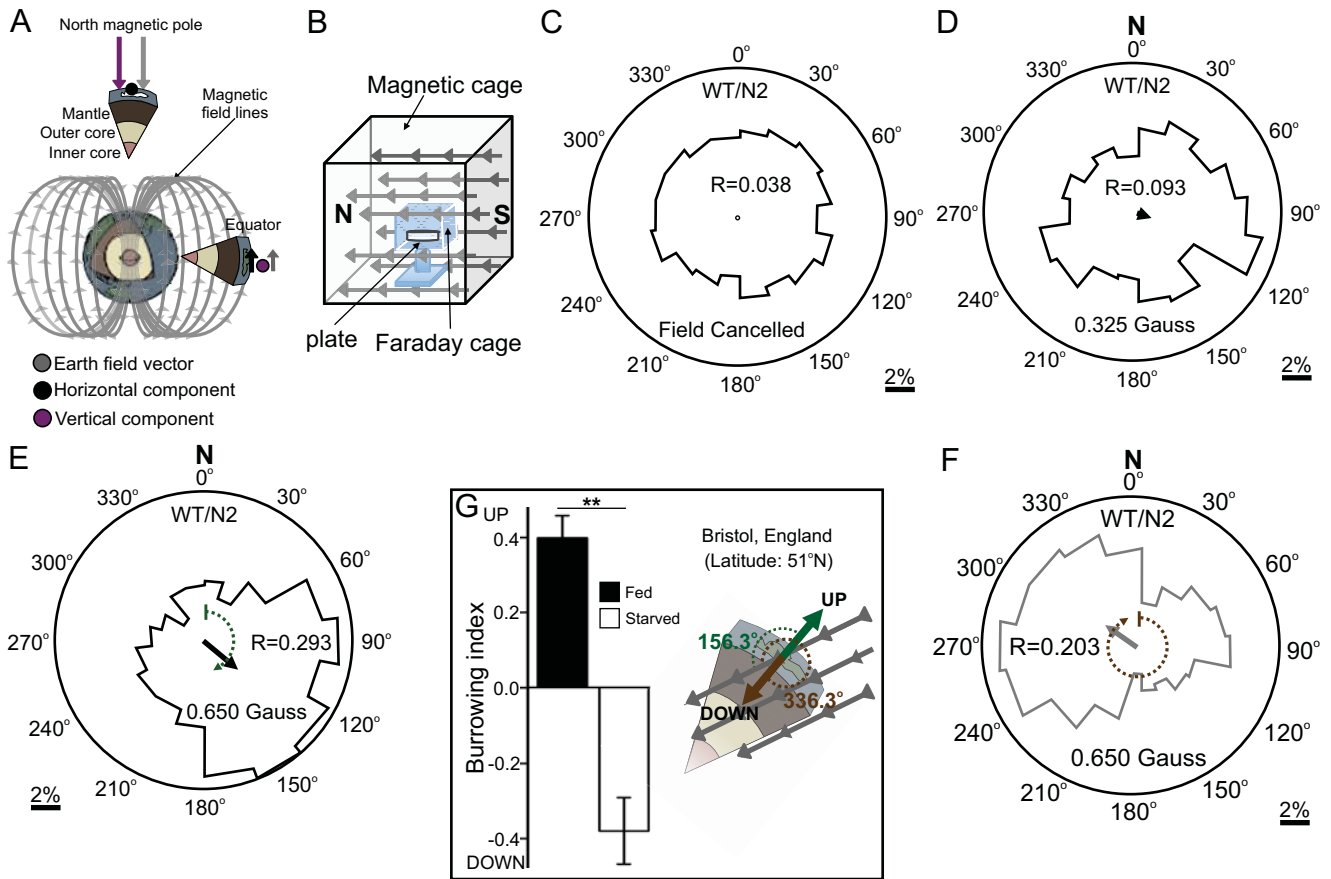
1078 **Figure 6-figure supplement 1. Genetic ablation of AFD does not impair**
1079 **chemotaxis.** (A) Genetic ablation of the AFD neurons did not impair the ability of worms
1080 to move, or orient to the chemical attractant diacetyl compared to control sister worms
1081 that did not carry a cell-death transgene (*ICE*). Comparison between the AFD neurons
1082 of animals expressing GFP (B), or GFP and ICE (C), revealed that in animals
1083 expressing the cell-death gene the AFD neuron is impaired and shows many of the
1084 typical signs of neurodegeneration (e.g. circular soma, beaded and fragmented
1085 processes).

1086

1087 **Figure 7-figure supplement 1. Measuring AFD calcium activity in partially and**
1088 **fully restrained worms.** (A) Worm-immobilization chip for high-resolution fluorescence
1089 microscopy. The two-level device consists of a valve layer (pink) sitting above a flow
1090 layer where the worms reside (grey). Animals enter the immobilization chamber via the
1091 worm input as fluid flow is directed to the fluid output. Small channels across the outer
1092 edge of the immobilization chamber permit fluid flow to pass but block the passage of
1093 the worms (left). As the flow pushes the worms against the outer edge of the chamber
1094 the valve layer is pressurized to fully immobilize the worms (right). A magnified view of a

1095 single animal pressed against the small channels along the outer edge of the
1096 immobilization chamber is shown during immobilization. (B) Alternatively, we partially
1097 restrained worms on an agar pad while measuring the brightness of the AFD (or AWC)
1098 sensory neurons before, during, and after exposure to a 60-Gauss magnetic stimulus.
1099 Images were taken only when the AFD soma was stationary. While consistent with our
1100 immobilized-worm experiments in sign (Figure 7), the amplitude of the responses were
1101 about ten times larger in partially restrained animals. (C) Expression of GCaMP3 in AFD
1102 neurons did not impair the worm's ability to orient to magnetic fields. * $P < 0.05$, ** $P <$
1103 0.001 . All values reported are means, and error bars represent S.E.M.





A
Adelaide, Australia
(Latitude: 34°S)

